Cellular/Molecular

Ca^{2+}/Calmodulin Disrupts AKAP79/150 Interactions with KCNQ (M-Type) K^+ Channels

Manjot Bal, Jie Zhang, Ciria C. Hernandez, Oleg Zaika, and Mark S. Shapiro
Department of Physiology, University of Texas Health Science Center at San Antonio, San Antonio, Texas 78229

M-type channels are localized to neuronal, cardiovascular, and epithelial tissues, where they play critical roles in control of excitability and K^+ transport, and are regulated by numerous receptors via $G_{q/11}$-mediated signals. One pathway shown for KCNQ2 and muscarinic receptors uses PKC, recruited to the channels by A-kinase anchoring protein (AKAP)79/150. As M-type channels can be variously composed of KCNQ1-5 subunits, and M current is known to be regulated by Ca^{2+}/calmodulin (CaM) and PIP_2, we probed the generality of AKAP79/150 actions among KCNQ1-5 channels, and the influence of Ca^{2+}/CaM and PIP_2 on AKAP79/150 actions. We first examined which KCNQ subunits are targeted by AKAP79 in Chinese hamster ovary (CHO) cells heterologously expressing KCNQ1-5 subunits and AKAP79, using fluorescence resonance energy transfer (FRET) under total internal reflection fluorescence (TIRF) microscopy, and patch-clamp analysis. Donor-dequenching FRET between CFP-tagged KCNQ1-5 and YFP-tagged AKAP79 revealed association of KCNQ2-5, but not KCNQ1, with AKAP79. In parallel with these results, CHO cells stably expressing M_1 receptors studied under perforated patch-clamp showed cotransfection of AKAP79 to "sensitize" KCNQ2/3 heteromers and KCNQ2-5, but not KCNQ1, homomers to muscarinic inhibition, manifested by shifts in the dose–response relations to lower concentrations. The effect on KCNQ4 was abolished by the T553A mutation of the putative PKC phosphorylation site. We then probed the role of CaM and PIP_2 in these AKAP79 actions. TIRF/FRET experiments revealed cotransfection of wild-type, but not dominant-negative (DN), CaM that cannot bind Ca^{2+}, to disrupt the interaction of YFP-tagged $AKAP79_{1\text{-}153}$ with CFP-tagged KCNQ2-5. Tonic depletion of PIP_2 by cotransfection of a PIP_2 phosphatase had no effect, and sudden depletion of PIP_2 did not delocalize GFP-tagged AKAP79 from the membrane. Finally, patch-clamp experiments showed cotransfection of wild-type, but not DN, CaM to prevent the AKAP79-mediated sensitization of KCNQ2/3 heteromers to muscarinic inhibition. Thus, AKAP79 acts on KCNQ2-5, but not KCNQ1-containing channels, with effects disrupted by calcified CaM, but not by PIP_2 depletion.

Introduction

A fundamental issue in cellular signaling is how focused signals are created that achieve specificity toward their relevant targets. A major mechanism involves clustering of the components of a signaling pathway into subcellular complexes by scaffolding proteins, such as A-kinase anchoring proteins (AKAPs) (Wong and Scott, 2004). One of the most pivotal AKAPs goes by the name AKAP79/150, from the molecular weight of its human and rodent orthologs, respectively (Hirsch et al., 1992), which appear to have identical roles across species. In addition to binding by PKA, AKAP79/150 binds calcineurin (CaN) (Coghlan et al., 1995), calmodulin (CaM) (Faux and Scott, 1997), phosphatidylinositol 4,5-bisphosphate (PIP_2) (Dell'Acqua et al., 1998), and protein kinase C (PKC) (Klauck et al., 1996), thus making it a point of convergence for integration of diverse signals. AKAP79/150 is involved of modulation of M-type (KCNQ, Kv7) K^+ channels. These voltage-gated channels are modulated by stimulation of several $G_{q/11}$-coupled receptors that activate PLC, hydrolyzing PIP_2 into cytoplasmic IP_3 and membrane-bound diacylglycerol (DAG). As for a plethora of other channels (Gamper and Shapiro, 2007a), KCNQ channels are sensitive to the abundance of PIP_2 in the membrane (Suh and Hille, 2002; Zhang et al., 2003; Li et al., 2005; Robbins et al., 2006; Suh et al., 2006; Hernandez et al., 2008), and certain receptors therefore suppress M current by depletion of PIP_2 (Delmas and Brown, 2005). In addition, M-type channels are also regulated by CaM in a Ca^{2+}-dependent manner, providing another mode of intracellular modulation (Gamper and Shapiro, 2003; Gamper et al., 2005a; Zaika et al., 2007; Bal et al., 2008). DAG is most famous for activation of several PKC isoforms. Although early studies suggested mammalian M current to not be sensitive to pharmacological activators or blockers of PKC (Hille, 1994), recent work indicates PKC to indeed act on KCNQ2 channels via recruitment of the kinase to the channels by AKAP79/150, which acts as a multiprotein complex with certain receptors, binding to KCNQ2 subunits and facilitating PKCβ phosphorylation of two serines on this channel (Hoshi et al., 2003, 2005). Recently, AKAP150 knock-out mice were used to show "sensitization" of neuronal M channels to muscarinic inhibition by AKAP150, as well as involvement in susceptibility to epileptic seizures (Tunquist et al., 2008).

Given that both AKAP79/150 and KCNQ channels are shared targets of several of the same signaling and/or regulatory mole-

Received Oct. 14, 2009; revised Dec. 15, 2009; accepted Dec. 20, 2009.

This work was supported by National Institutes of Health–National Institute of Neurological Disorders and Stroke Grants R01 NS43394 and ARRA R01 NS065138 and by American Heart Association Grant-in-Aid 0755071Y to M.S.S. We thank Pamela Reed for expert technical assistance. We are also grateful for many helpful discussions with Björn Falkenburger, David Brown, Bertil Hille, and Mark Dell'Acqua. We also thank Mark Dell'Acqua for several AKAP79 clones used in this study.

Correspondence should be addressed to Mark S. Shapiro, Department of Physiology, MS 7756, University of Texas Health Science Center at San Antonio, 7703 Floyd Curl Drive, San Antonio, TX 78229. E-mail: shapirom@uthscsa.edu.

DOI:10.1523/JNEUROSCI.5175-09.2010

 0270-6474/10/302311-13$15.00/0

cules, we set out to probe their molecular interactions. We particularly focused on the role of CaM in regulating the physical and functional association of AKAP79 with KCNQ channels and in the possible role of PIP_2 in facilitating AKAP79/150 localization to the membrane and its action on the channels. We first asked whether the role of AKAP79/150 is specific to KCNQ2, or rather whether it generalizes to other KCNQ subunits as well. To probe the physical interactions in individual living cells, we used fluorescence resonance energy transfer under total internal reflection fluorescence microscopy. The functional studies used patch-clamp electrophysiology on mammalian cells heterologously transfected with specific KCNQ subunits and signaling molecules. We find AKAP79 to act on four of five KCNQ subunit types, and that functional CaM, but not PIP_2 depletion, severely disrupts the association and action of AKAP79 on M-type channels.

Materials and Methods

cDNA constructs. Human KCNQ1-5 (GenBank accessions AAC51781, AF110020, AF071478, AF105202, and AF249278, respectively) were given to us by Michael Sanguinetti (KCNQ1, University of Utah, Salt Lake City, UT), David McKinnon (KCNQ2, SUNY, Stony Brook, NY), Thomas Jentsch (KCNQ3, KCNQ4, Zentrum fur Molekulare Neurobiologie, Hamburg, Germany), and Klaus Steinmeyer (KCNQ5, Aventis Pharma, Frankfurt am Main, Germany). The plasmids for AKAP79, GFP-tagged AKAP79, and $AKAP79_{1-153}$ were kindly given to us by Mark Dell'Acqua (University of Colorado, Denver, CO). We thank John Scott (Oregon Health & Science University, Portland, OR) for kindly sharing the clone for AKAP150. Plasmids were subcloned into pECFP-N1 or pEYFP-N1 (Clontech) or pcDNA3.1 (Invitrogen) vectors using standard techniques. The membrane-localized CFP-YFP tandem construct (Rho-pYC) was kindly given to us by Paul Slesinger (Salk Institute). It consists of the C-terminal prenylation site of Rho (RQKKRRGCLLL) appended to the C terminus of a YFP-CFP fusion (Fowler et al., 2007). The KCNQ4 (T553A) mutation was made by QuikChange PCR (Stratagene).

Cell culture and cDNA transfections. Chinese hamster ovary (CHO) cells were grown in 100 mm tissue culture dishes (Falcon) in DMEM medium with 10% heat-inactivated fetal bovine serum plus 0.1% penicillin and streptomycin in a humidified incubator at 37°C (5% CO_2) and passaged about every 4 d. Cells were discarded after ~30 passages. For the total internal reflection fluorescence (TIRF)/fluorescence resonance energy transfer (FRET) and confocal translocation experiments, cells were first passaged onto 35 mm plastic tissue-culture dishes and transfected 24 h later with Polyfect reagent (QIAGEN), according to the manufacturer's instructions and as previously described (Gamper et al., 2005b). The next day, cells were plated onto poly-L-lysine-coated glass-bottomed 35 mm tissue-culture dishes (MatTek) or coverglass chips, and experiments performed over the following 1–2 d.

TIRF microscopy. Fluorescence emissions from enhanced cyan fluorescent protein (CFP)-tagged or enhanced yellow fluorescent protein (YFP)-tagged KCNQ1-5 channels were collected at room temperature using TIRF (also called evanescent field) microscopy (Axelrod, 2003). TIRF illumination involves directing a laser beam at the interface between two transparent media of differing refractive indices at a glancing angle. In this case, the two refractive media are the glass coverslip and the cytoplasm. By the laws of optics, at an angle greater than the critical angle determined by the ratio of the two refractive indices, the light beam is not primarily transmitted to the second medium, but is instead reflected; however, not all the light energy is reflected; a component penetrates into the second medium as an "evanescent wave" that decays exponentially in intensity over a distance of only several hundred nanometers. All TIRF experiments were performed in the total internal reflection fluorescence microscopy core facility housed within the Department of Physiology. Fluorescence emissions were collected using an inverted TE2000 microscope with through-the-lens (prismless) TIRF imaging (Nikon). This system is equipped with a vibration isolation system (Technical Manufacturing) to minimize drift and noise. Samples were viewed through a plan-Apo TIRF 60× oil-immersion high resolution (1.45 numerical aperture) TIRF objective. Coupled to the microscope is a laser light delivery system (Prairie Technologies) consisting of a 40 mW argon laser outputting 488 and 514 nm lines and a 442 nm diode pumped solid-state laser. The excitation light was selected with an acoustic optical tunable filter, controlled by MetaMorph software running on a PC. CFP and YFP emissions were simultaneously collected using the Dual-View chip splitter (Optical Insights), equipped with a filter cube containing HQ470nm/30m and HQ550nm/30m emission filters for CFP and YFP emission, respectively, and a 505 nm dichroic mirror for separation of emission wavelengths. In this configuration, the microscope uses only a dual-bandpass TIRF dichroic mirror to separate the excitation and emission light, with no excitation filters in the microscope cube. The TIRF angle was adjusted by eye to give the signature TIRF illumination to the experimental chamber. Fluorescence images were collected and processed with a 16 bit, cooled charge-coupled device camera (Cascade 512F; Roper Scientific) interfaced to a PC running MetaMorph software. This camera uses a front-illuminated EMCCD with on-chip multiplication gain. Images were collected (200–600 ms exposure time, adjusted to best exploit the dynamic range of the camera without pixel saturation) immediately before and after photobleaching. Images were not binned or filtered, with pixel size corresponding to a square of 122 × 122 nm.

FRET. We used either the "acceptor photobleaching" (donor dequenching) or "sensitized emission" method of evaluating FRET efficiency. In the former, the emission of the donor fluorophore is compared before and after photobleaching of the acceptor (Centonze et al., 2003). YFP photobleaching was performed using the 100 W mercury lamp of the microscope, using a standard YFP filter cube. We find that 5–7 min excitation by the mercury lamp using the YFP cube is sufficient to photobleach >75% of the YFP fluorophores, yet results in negligible photobleaching of the CFP fluorophores. The following protocol was used: The medium in the glass-bottomed dishes was exchanged with Ringer's solution that contained the following (in mM): 160 NaCl, 5 KCl, 1 $MgCl_2$, 2 mM $CaCl_2$, and 10 HEPES, pH 7.4 with NaOH. Cells were first examined using the mercury lamp and standard CFP or YFP filter cubes to find a suitable cell robustly expressing both CFP- and YFP-tagged proteins. Under TIRF illumination, the focal plane used is critical, and was adjusted if necessary immediately before each image acquisition to obtain a sharp TIRF image. The focusing and cell-centering protocol resulted in CFP photobleaching of <1%. TIRF images using 442 and 514 laser lines were acquired before and after photobleaching of the YFP fluorophores. %FRET was calculated as the percentage increase in CFP emission after YFP photobleaching by using the following formula: $\%FRET = [(CFP_{post} - CFP_{pre})/CFP_{pre}] \times 100$, where CFP_{post} is CFP emission after YFP photobleaching, and CFP_{pre} is CFP emission before YFP photobleaching. The %FRET was calculated by drawing regions of interest around the entire area of the cell and subtracting the background in a cell-free region for each image.

For measurement of TIRF/FRET using the "sensitized emission" method, the sample was excited at 442 nm, and CFP and YFP emission simultaneously collected using the Dual-View/camera combination, where the split sides of the camera chip will be referred to as the CFP and the YFP channels, respectively. To quantify the effective FRET efficiency for each experiment, we use the "3-cube" method used by many investigators (Sorkin et al., 2000; Erickson et al., 2001; Oliveria et al., 2003; Zheng and Zagotta, 2004), based on the formalism of Gordon et al. (1998). Our system does not use three physical "cubes," but rather the Dual-View; however, the principle, which we outline here, is the same. To quantify the "bleed-through" of the CFP emission into the YFP channel, cells expressing only ECFP-M were excited at 442 nm, and the image intensities of the cell on the CFP and YFP channels quantified, yielding a ratio of YFP channel/CFP channel of 26%. By exciting cells only expressing EYFP-M, we determined that the bleed-through of YFP emission into the CFP channel is zero, as is the excitation of CFP by 514 nm light. The direct excitation of YFP at 442 nm is calculated as a ratio of YFP excitation at 514 nm, and this was quantified using cells only expressing EYFP-M, yielding a value of 4.3%. Thus, to measure sensitized-emission FRET, the cells are sequentially imaged under 442 and 514 nm laser lines under TIRF. The intensity of the cell region in the YFP channel is first

scaled down by 26% of the intensity of the identical cell region in the CFP channel, to isolate the YFP emission. The total YFP emission is then broken down into that arising from direct excitation by the 442 nm light, and that from energy transfer from CFP. The former is calculated by multiplying the 514 nm image in the YFP channel by 4.3%, with the remainder thus assumed due to FRET. We then calculate the ratio of total YFP emission to that from direct excitation of YFP, the "FRET ratio" (FR). The FR value is easily converted to FRET efficiency (E_{eff}) using the following equation: $E_{eff} = (FR - 1) \times (\varepsilon_{YFP,442}/\varepsilon_{CFP,442})$, where $\varepsilon_{YFP,442}$ and $\varepsilon_{CFP,442}$ are the molar extinction coefficients for YFP and CFP when excited at 442 nm. From their published maximal molar extinction coefficients and known excitation spectra of YFP and CFP (Patterson et al., 2001), the $\varepsilon_{YFP,442}/\varepsilon_{CFP,442}$ ratio was calculated to be 0.101, which is used to convert the FR to FRET efficiency.

Live-cell confocal microscopy. For the confocal "translocation" experiments, we used the Nikon Swept-Field Confocal located in the confocal microscopy core facility in the Department of Physiology. This rig consists of a TE200E2 inverted motorized microscope system and the Prairie Technologies Livescan SFC capable of slit-scan confocal (up to 120 frames/s) or pinhole-mode swept field confocal (up to 40 frames/s) and choice of CoolSnap HQ2 or Cascade II cameras. The system has a 440 nm blue diode laser and an argon laser outputting 488 and 514 nm laser lines for excitation of CFP, GFP, and YFP, respectively. Solution exchange is by activation of solenoid valves, and images acquired and analyzed using Nikon Elements software running on a PC.

Immunostaining and confocal analysis. Cells were transfected with EGFP and AKAP150, grown on poly-L-lysine-coated coverslips, in 4% paraformaldehyde, washed twice with 100 mM sodium phosphate (PB, pH 7.4), three times with PB + 150 mM NaCl (PBS), and blocked with 5% goat serum and 0.1% saponin in PBS (PBS + GS). The cells were incubated for 3 h at room temperature with primary goat anti-AKAP150 (Santa Cruz Biotechnology) antibody diluted 1:2000 in PBS + GS. Cells were washed six times with PBS and then incubated with goat Rhodamine Red-conjugated anti-goat secondary antibody (1:500, Jackson ImmunoResearch) in PBS + GS for 1 h. Cells were then washed three times with PBS, twice with PB, and three times with water. Air-dried slides were mounted on a drop of Vectashield (Vector Laboratory) and sealed with nail polish. Stained cells were viewed with an Olympus FV-500 confocal microscope in the Optical Imaging Core Facility, using the lasers and excitation/emission filters appropriate for GFP and Rhodamine Red. Since GFP was used as a reporter for successful transfection, images were collected in "sequential" mode to avoid bleed-through of the GFP (green) and Rhodamine (red) signals. Single images were collected 3–5 μm above the surface of the coverslip.

Perforated-patch electrophysiology. Pipettes were pulled from borosilicate glass capillaries (1B150F-4, World Precision Instruments) using a Flaming/Brown micropipette puller P-97 (Sutter Instruments) and had resistances of 1–4 MΩ when filled with internal solution and measured in standard bath solution. Membrane current was measured with pipette and membrane capacitance cancellation, and sampled at 5 ms and filtered at 1 kHz by an EPC-9 amplifier, and PULSE software (HEKA/Instrutech). In all experiments, the perforated-patch method of recording was used with amphotericin B (600 μg/ml) in the pipette (Rae et al., 1991). Amphotericin was prepared as a stock solution as 60 mg/ml in DMSO. In these experiments, the access resistance was typically 10 MΩ 5–10 min after seal formation. Cells were placed in a 500 μl perfusion chamber through which solution flowed at 1–2 ml/min. Inflow to the chamber was by gravity from several reservoirs, selectable by activation of solenoid valves (Warner Scientific). Bath solution exchange was essentially complete by <30 s. Experiments were performed at room temperature.

Reagents. Oxotremorine methiodide (Sigma); DMEM, fetal bovine serum, penicillin/streptomycin (Invitrogen); amphotericin B (Calbiochem); XE991 (Tocris Biosciences).

Results

We studied the interaction with M-type KCNQ channels of an AKAP that goes by the name AKAP79/150, from the molecular weight of its human and rodent orthologs, respectively, with the bovine ortholog named AKAP75 (Hirsch et al., 1992). The Gene Nomenclature Committee has named the gene AKAP5; however, in this paper, we will use the more established AKAP79/150 nomenclature when talking about the AKAP5 gene product in general, and use the ortholog-specific name when appropriate. Previous work using coimmunoprecipitation and GST pull-down analyses has indicated binding of AKAP150 to KCNQ2 (Hoshi et al., 2003). We sought to examine the interaction between AKAP79/150 and KCNQ channels in the milieu of individual living cells. For this purpose our main techniques were FRET (Sekar and Periasamy, 2003) and perforated-patch voltage clamp of mammalian cells. We used the widely used FRET pair of enhanced CFP and enhanced YFP, fused to KCNQ1-5 channels and either full-length AKAP79, or its proximal 153 residues, at the carboxy end of the proteins in all cases. We will call these constructs KCNQx-CFP and AKAP79-YFP, respectively.

FRET was measured in CHO cells, visualized under TIRF microscopy (Axelrod, 2003), in which we can selectively excite only fluorophores located within ~300 nm of the plasma membrane of the cell (Steyer and Almers, 2001). Our previous work indicates that the illumination of cytoplasmic fluorophores is extremely low, thus isolating events in the membrane where reside the KCNQ channels and AKAP79 molecules of interest (Bal et al., 2008). The bulk of these measurements used the "donor-dequenching" (acceptor-photobleaching) method, in which the emission from the donor (CFP) is compared before and after photobleaching of the acceptor (YFP). We initially performed control experiments using the Rho-pYC construct consisting of a membrane-targeted fusion of CFP and YFP (Fowler et al., 2007) to assess the suitability of the TIRF/FRET method for our requirements. In the donor-dequenching method, FRET efficiency is calculated as the percentage increase in CFP emission after YFP photobleaching by using the following formula: $\%FRET = [(CFP_{post} - CFP_{pre})/CFP_{pre}] \times 100$, where CFP_{post} and CFP_{pre} are the CFP emissions after and before YFP photobleaching, respectively. Further details are described in Materials and Methods. The FRET efficiency for the Rho-pYC construct was 26.0 ± 1.2% (n = 18). Our negative control was coexpression of AKAP79-YFP with a membrane-targeted CFP (ECFP-M), which yielded a FRET value of only 1.9 ± 2% (n = 13) (Fig. 1*B*). Since the expression of ECFP-M is quite high, we take this low value as an upper limit for the "spurious" FRET due to incidental proximity for the experiments in our system.

AKAP79 interacts with KCNQ2-5, but not KCNQ1, channels

Our first question was to ask which KCNQ subunits interact with AKAP79/150. In this study, we assume that the actions of AKAP79 or 150 orthologs are identical, and so used AKAP79 in these experiments. CHO cells were transfected with CFP-tagged KCNQ1-5 channels and AKAP79-YFP, and the FRET measured by the donor-dequenching method under TIRF illumination. Shown in Figure 1*A* are TIRF images of CFP and YFP emission, before and after selective photobleaching of YFP, displayed in "rainbow" and yellow pseudocolor, respectively. The CFP emission was significantly greater after YFP photobleach for KCNQ2-5, but not for KCNQ1. These data are summarized in Figure 1*B*. For KCNQ2-5, the FRET was 15.8 ± 1.7% (n = 18), 14.9 ± 1.9% (n = 14), 12.2 ± 2.7% (n = 14), and 13.7 ± 1.6% (n = 16), respectively. However, for KCNQ1, the FRET was only 4.8 ± 1.6% (n = 14), which was not significantly greater than the FRET of AKAP79-YFP with the ECFP-M control. Thus, AKAP79 intimately associates with KCNQ2-5, but not with KCNQ1, consistent with the role of a different AKAP,

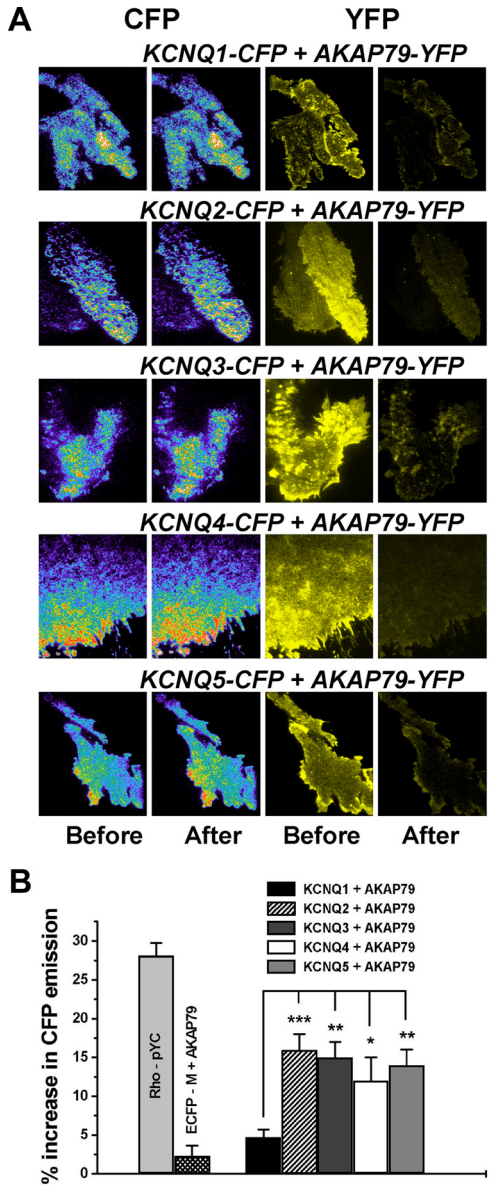

Figure 1. KCNQ2-5, but not KCNQ1, interacts with AKAP79. ***A***, Shown are images of CHO cells under TIRF illumination expressing CFP-tagged KCNQ1-5 and YFP-tagged AKAP79, using 442 or 514 nm laser lines. Images of the CFP (left, in rainbow pseudocolor) and YFP (right, in yellow pseudocolor) emissions are shown before or after YFP photobleach, as labeled. Note the brighter CFP emission (warmer colors) after YFP photobleach for KCNQ2-5, but not KCNQ1. ***B***, Bars shows the percentage increase in CFP emission after YFP photobleach for the groups in ***A***, as well as for the membrane-targeted CFP-YFP tandem (Rho-pYC) and for ECFP-M + AKAP79-YFP that serve as our positive and negative FRET controls, respectively. $*p < 0.05$, $**p < 0.01$, $***p < 0.001$.

Yotiao, in mediating phosphorylation of KCNQ1-containing channels (Chen et al., 2005). It is important to note that whereas the earlier work suggested this interaction using the *in vitro* methods of co-IP and pull-down assays, these data indicate it in individual living cells.

AKAP79 "sensitizes" KCNQ2-5, but not KCNQ1, channels to inhibition by muscarinic receptors

The FRET experiments presented so far indicate intimate association between AKAP79 and KCNQ2-5, but not KCNQ1, channels. To determine whether muscarinic suppression of the currents from these channels are influenced by the presence or absence of AKAP79/150, we performed patch-clamp experiments on CHO cells transfected with homomeric or heteromeric KCNQ1-5 channels. Since PKC phosphorylation mediated by AKAP79/150 was shown to "sensitize" M channels to muscarinic stimulation of sympathetic neurons, manifested as a shift in the dose–response curve of current depression versus agonist to lower concentrations (Hoshi et al., 2003), we performed similar assays on the cloned channels to probe the functional specificity of AKAP79 action. In this paradigm, a shift of the dose–response relationship to lower concentrations of agonists in cells in which AKAP79 is coexpressed indicates a functional interaction.

We first examined the influence of AKAP79 on the heteromeric KCNQ2/3 channels expressed in CHO cells, which immunoblot analysis indicates express nearly undetectable levels of endogenous AKAP150 (data not shown). In these experiments, CHO cells stably expressing $G_{q/11}$-coupled M_1 receptors were cotransfected with KCNQ2 and KCNQ3, together either with only GFP or with GFP-tagged AKAP79, and studied under perforated-patch voltage clamp. The suppression of the KCNQ2/3 current was measured over a range of concentrations of the muscarinic agonist, oxotremorine methiodide (oxo-M). In cells cotransfected with GFP-tagged AKAP79, oxo-M induced a larger suppression of the current at all concentrations tested, compared with cells cotransfected only with GFP (Fig. 2*A*,*B*). These data are summarized in Figure 2*C* as a dose–response relation of KCNQ2/3 current inhibition versus [oxo-M]. For cells transfected with KCNQ2 and KCNQ3, together with GFP or with GFP-tagged AKAP79, the oxo-M concentrations that induced half-maximum inhibition of the current (IC_{50}) were 0.77 ± 0.05 μM ($n = 7$), and 0.16 ± 0.01 μM ($n = 8$), respectively. There was no difference in the suppression of the current at saturating [oxo-M], which was ~98% in both groups of cells. Thus, AKAP79 "sensitizes" suppression of the heteromeric KCNQ2/3 current to stimulation of muscarinic receptors, presumably by mediating phosphorylation of the channel by PKC, consistent with the role of AKAP79/150 in facilitating muscarinic suppression of neuronal M current (Hoshi et al., 2003, 2005; Tunquist et al., 2008).

We then performed similar experiments for KCNQ1-5 homomers. For KCNQ3, we used the (A315T) mutant that yields much larger currents than wild-type (WT) KCNQ3, yet still exhibits high single-channel open probability and high apparent affinity for PIP_2 (Zaika et al., 2008; Hernandez et al., 2009). In these experiments, cells were transfected individually with KCNQ1-5, together either with only GFP or with GFP-tagged AKAP79. We found cotransfection of GFP-tagged AKAP79 to shift the dose–response relationships for KCNQ2-5, but not KCNQ1, to lower concentrations of oxo-M (Fig. 3*B*–*E*). For KCNQ2-5 channels cotransfected with only GFP, the IC_{50} of oxo-M were 0.32 ± 0.03 μM ($n = 6$), 1.3 ± 0.2 μM ($n = 7$), 0.09 ± 0.01 μM ($n = 7$), and 0.51 ± 0.02 μM ($n = 4$), respectively. Coexpression of GFP-tagged AKAP79 shifted their dose–response relations to lower concentrations of oxo-M, for which the IC_{50} were 0.065 ± 0.008 μM ($n = 7$), 0.61 ± 0.07 μM ($n = 6$), 0.03 ± 0.01 μM ($n = 5$), and 0.16 ± 0.02 μM ($n = 5$), respectively. However, suppression of KCNQ1 currents was not affected by the presence or absence of AKAP79 (Fig. 3*A*). For cells cotransfected with GFP only, the IC_{50} for oxo-M was 0.75 ± 0.11 μM ($n = 6$), not significantly different from that in cells cotransfected with GFP-tagged AKAP79, 0.89 ± 0.07 μM ($n = 6$). For KCNQ2, KCNQ4, and KCNQ5, there was no effect of AKAP79 on the suppression of the current at saturating [oxo-M], which was 94–99%. However, for KCNQ3 (A315T) channels, coexpression of AKAP79 not only shifted the dose–response curve to the left, but

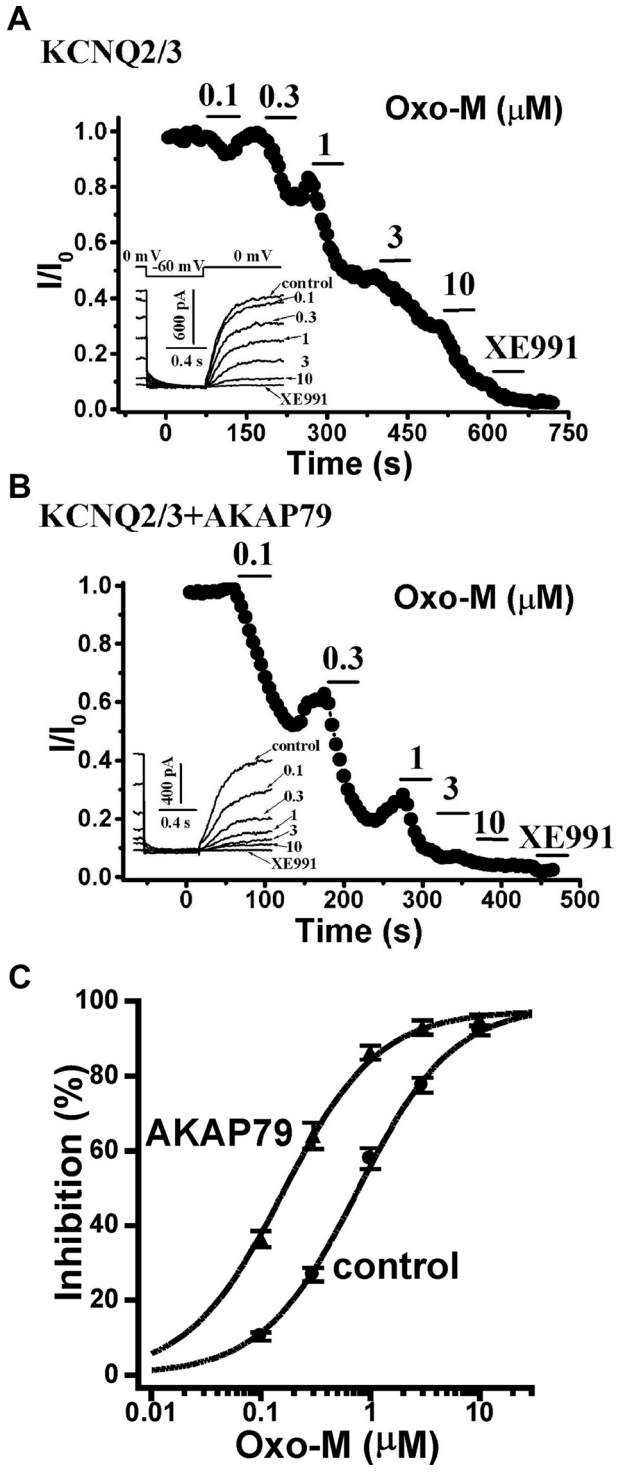

Figure 2. AKAP79 sensitizes KCNQ2/3 channels to inhibition by muscarinic receptor stimulation. Plotted are normalized KCNQ2/3 currents during the experiment from stably M_1-expressing CHO cells transfected with KCNQ2 + 3 and GFP only (***A***) or together with GFP-tagged AKAP79 (***B***), while a range of concentrations of oxo-M or 10 μM XE991 were bath applied, as indicated by the bars. Representative current traces are shown in the insets, using the indicated voltage protocol. ***C***, Plotted are the summarized dose–response relation of the KCNQ2/3 current versus oxo-M concentration for cells transfected with KCNQ2 + 3 and GFP only (control) or together with GFP-tagged AKAP79. The data were fit by Hill equation curves, with the parameters given in the text.

also increased the maximal inhibition, from 59 ± 4% ($n = 7$) in control cells, to 94 ± 2% ($n = 6$) in cells cotransfected with GFP-tagged AKAP79, a result explained by the high PIP_2 affinity of KCNQ3 channels (Hernandez et al., 2009) (see Discussion). Finally, the action of AKAP150 on KCNQ2 channels has been suggested to be due to their phosphorylation by PKC at two serines at positions 534 and 541. Both KCNQ4 and KCNQ5 possess alanines analogous to S534 of KCNQ2, but both possess threonines analogous to S541; thus, we examined KCNQ4 (T553A) and KCNQ5 (T506A). The latter did not express functional currents, but the former yielded robust currents that were not sensitive to the presence of AKAP79, and had IC_{50} values for muscarinic suppression that were not different from that of WT KCNQ4. For cells transfected with KCNQ4 (T553A) and GFP only, or with GFP-tagged AKAP79, the IC_{50} values were 0.083 ± 0.009 μM ($n = 7$) and 0.066 ± 0.008 ($n = 8$), respectively, and the suppression at maximal [oxo-M], 94–96%, was not affected (Fig. 3*D*). Thus, phosphorylation of a sole threonine in KCNQ4 is sufficient for the sensitization effect of AKAP79 on muscarinic suppression of the KCNQ4 current.

Functional calmodulin disrupts the interactions between $AKAP79_{1\text{-}153}$ and KCNQ2-5 channels

The proximal 153 residues of AKAP79 contain the A, B, and C domains, which all contribute to binding of CaM and PIP_2 (Faux and Scott, 1997; Dell'Acqua et al., 1998), as well as the proximal 143 residues shown to be sufficient for binding to KCNQ2 (Hoshi et al., 2003). In addition, the C-terminal region of KCNQ2 channels shown to be involved in binding of AKAP150 (Hoshi et al., 2003) also contains dual sites where CaM binds to the channels (Wen and Levitan, 2002; Yus-Najera et al., 2002; Gamper and Shapiro, 2003; Haitin and Attali, 2008). Thus, we suspected that CaM could be involved in regulating the interaction of AKAP79/150 with KCNQ channels, by CaM binding either to the channel, to AKAP79/150, or to both. Thus, we performed TIRF/FRET experiments to probe the effect of CaM expression on channel/AKAP79 interactions. In these experiments, the acceptor construct consisted of YFP fused to the end of the proximal 153 residues of AKAP79 ($AKAP79_{1\text{-}153}$). We also sought to distinguish between the actions of Ca^{2+}-free CaM (apoCaM) and calcified CaM. Thus, CHO cells were cotransfected with CFP-tagged KCNQ2-5 channels, $AKAP79_{1\text{-}153}$-YFP and either WT or a dominant-negative (DN) CaM in which all four Ca^{2+}-binding sites have been mutated, rendering CaM unable to bind Ca^{2+} (Geiser et al., 1991; Gamper and Shapiro, 2003; Gamper et al., 2005a).

In cells cotransfected with CFP-tagged KCNQ2 and $AKAP79_{1\text{-}153}$-YFP, there was robust FRET, consistent with the results using full-length AKAP79. However, when cells were cotransfected with WT CaM, but not with DN CaM, the FRET was much less (Fig. 4*A*). For cells transfected with CFP-tagged KCNQ2 and $AKAP79_{1\text{-}153}$-YFP, or together with WT or DN CaM, the FRET efficiencies were 12.6 ± 1.3% ($n = 25$), 5.1 ± 1.9% ($n = 13$, $p < 0.001$), and 11.7 ± 1.2% ($n = 11$), respectively (Fig. 5). These data are particularly interesting since the site of Ca^{2+}/CaM binding to KCNQ channels overlaps that of AKAP79/150 binding, and since the A-domain of AKAP79 necessary for PKC binding is also important for interactions of AKAP79/150 with Ca^{2+}/CaM. Is the CaM effect due to CaM action on the channel or on the AKAP? Figure 4*A* shows one test, in which FRET was evaluated in the KCNQ2 (R345E) mutant that does not bind CaM, as shown by *in vitro* (Wen and Levitan, 2002) and live-cell TIRF/FRET (Bal et al., 2008), assays. The FRET between KCNQ2 (R345E) and $AKAP79_{1\text{-}153}$ was strong, and was not reduced when the cell was cotransfected with WT CaM. For cells expressing CFP-tagged KCNQ2 (R345E) and $AKAP79_{1\text{-}153}$-YFP alone or together with WT CaM, the FRET was 14.7 ± 3.6% ($n =$

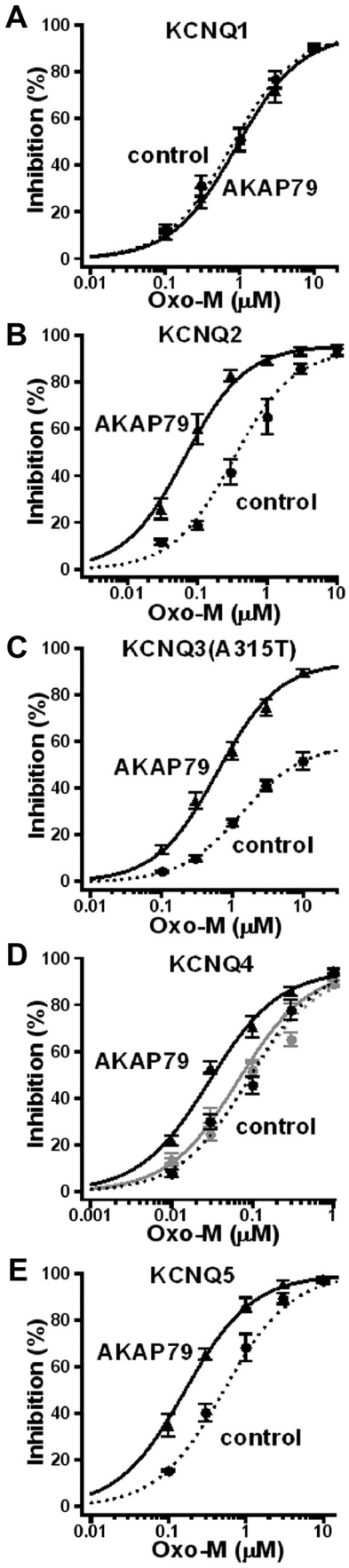

Figure 3. AKAP79 sensitizes KCNQ2-5, but not KCNQ1, channels to inhibition by muscarinic receptor stimulation. Plotted are the summarized inhibition of the current versus oxo-M concentration for M_1-expressing CHO cells transfected with KCNQ1 (***A***), KCNQ2 (***B***), KCNQ3 (A315T) (***C***), KCNQ4 (WT or the T553A mutant) (***D***), or KCNQ5 (***E***), either with GFP only (control, circles) or together with GFP-tagged AKAP79 (AKAP79, triangles). The data were fit by Hill equation curves, with the parameters given in the text. For all, the dotted or solid curves are the fits to the control or AKAP79 data, respectively, and in ***D***, the gray symbols and curves represent the data from the KCNQ4 (T553A) mutant.

12) and 19.8 ± 4.9% ($n = 13$), respectively (Fig. 5). These data suggest that CaM interferes with AKAP79 interactions with KCNQ2 channels by competing for an overlapping binding site on the channel, not due to its binding to AKAP79.

We also performed TIRF/FRET measurements using a "sensitized emission" paradigm, in which FRET is assayed as the additional emission from YFP due to energy transfer from CFP. In this paradigm, this YFP signal must be corrected by a number of controls, most importantly the "bleed-through" of the CFP signal into the YFP channel, and the "direct excitation" of YFP by the 442 nm light used to excite CFP in our system. The specifics of our modified "3-cube FRET" approach can be found in Materials and Methods. For the Rho-pYC control, the sensitized-emission FRET was 27.3 ± 1.7% ($n = 15$) and for CFP-tagged KCNQ2 and $AKAP79_{1-153}$-YFP, it was 14.1 ± 3.7% ($n = 17$) (Fig. 5). Both of these values are very similar to those obtained using the donor-dequenching paradigm. Since the sources of artifact for these two methods are distinct (Hoppe et al., 2002; Zal and Gascoigne, 2004), the congruence of our FRET values using the two methods should give confidence to our results. We also assayed the FRET between KCNQ2-CFP and a YFP-tagged AKAP79 lacking the proximal 74 residues shown previously to not significantly disrupt AKAP79 membrane localization (Dell'Acqua et al., 1998). However, donor-dequenching FRET between KCNQ2-CFP and $AKAP79_{(\Delta 1-74)}$-YFP was reduced to only 6.9 ± 1.8% ($n = 11$, $p < 0.01$) (Fig. 5) (supplemental Fig. 1, available at www.jneurosci.org as supplemental material), suggesting that membrane localization, per se, does not suffice for interactions with KCNQ channels.

We then asked whether CaM expression had the same effect for the interaction between $AKAP79_{1-153}$ and KCNQ3-5. Cells were transfected with CFP-tagged KCNQ3, KCNQ4 or KCNQ5 and $AKAP79_{1-153}$-YFP, either alone or together with WT or DN CaM. For all three subunit types, the CFP emission was significantly brighter after photobleaching of YFP, indicating interaction between $AKAP79_{1-153}$ and KCNQ3, KCNQ4, and KCNQ5 (Fig. 4*B–D*). The mean FRET efficiencies were 8.8 ± 2.2% ($n = 11$), 10.1 ± 1.7% ($n = 14$), and 11.6 ± 2.1% ($n = 12$), respectively (Fig. 5). As for the action on interactions with KCNQ2, coexpression of WT, but not DN CaM, disrupted the interactions with KCNQ3-5 as well. For cells coexpressing WT CaM, the FRET efficiencies were 2.1 ± 1.6% ($n = 14$, $p < 0.01$), 3.1 ± 1.0% ($n = 10$, $p < 0.01$), and 6.8 ± 0.8% ($n = 23$, $p < 0.01$), respectively, and for cells coexpressing DN CaM, they were 15.0 ± 1.5% ($n = 13$,), 14.7 ± 2.4% ($n = 13$), and 14.7 ± 1.6% ($n = 12$), respectively (Fig. 5). These data suggest an interaction of $AKAP79_{1-153}$ with all three of these channel types that is significant, and disrupted by WT, but not DN CaM. They also suggest that the proximal 153 residues of AKAP79 suffice for interactions with KCNQ3-5 channels as well (the difference for KCNQ3 between full-length AKAP79 and $AKAP79_{1-153}$ was not significant at the $p < 0.05$ level).

In the donor-dequenching paradigm, the measured FRET efficiency can be affected by variations in fractional occupancy of the donor-tagged molecule by the acceptor-tagged molecule, an

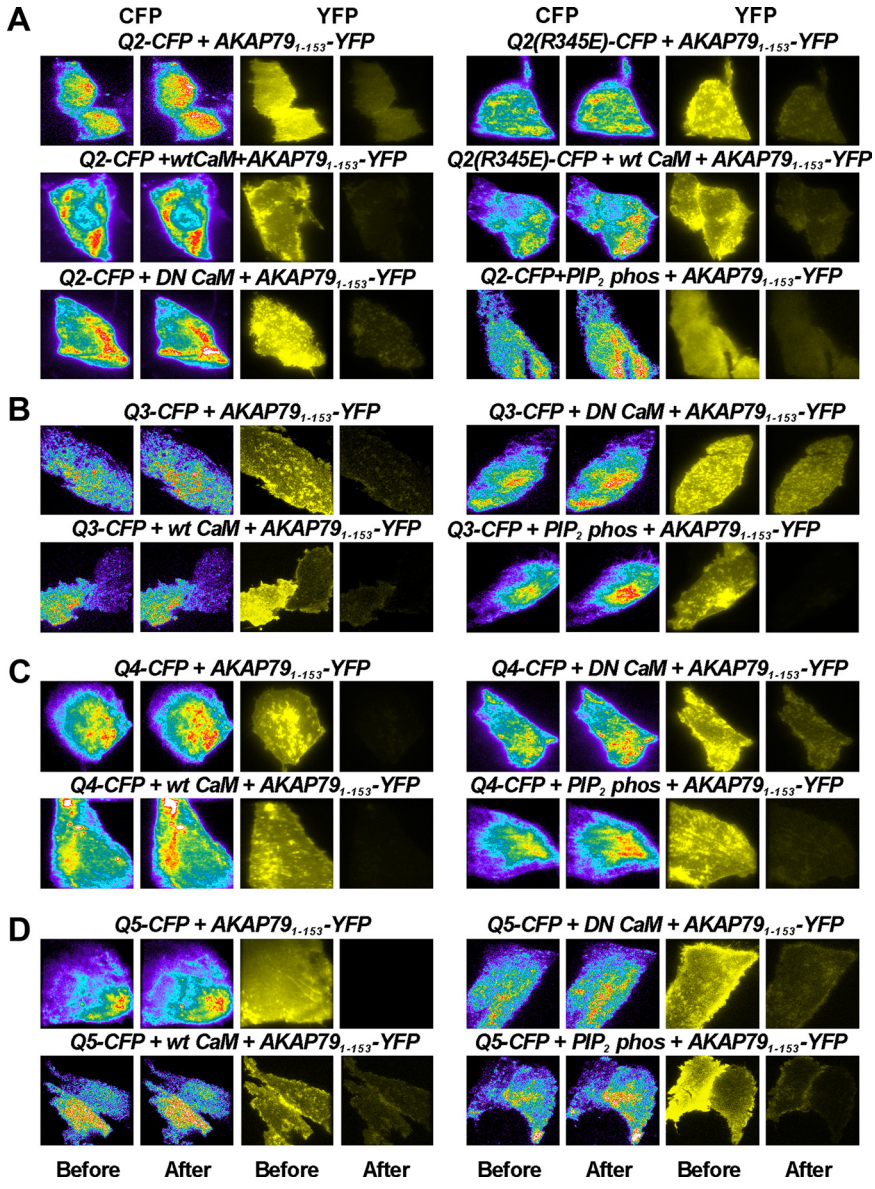

Figure 4. Functional Ca^{2+}/CaM, but not PIP_2 depletion, disrupts the interaction between KCNQ2-5 channels and AKAP79$_{1-153}$. Shown are images of CHO cells under TIRF illumination expressing YFP-tagged AKAP79$_{1-153}$ and CFP-tagged KCNQ2 (*Q2*, WT or the R345E mutant) (***A***), KCNQ3 WT (*Q3*) (***B***), KCNQ4 (*Q4*) (***C***), or KCNQ5 (*Q5*) (***D***), either alone or together with WT CaM, dominant-negative (*DN*) CaM or a PIP_2 phosphatase (*PIP_2 phos*), using 442 or 514 nm laser lines. Images of the CFP (rainbow pseudocolor) and YFP (yellow pseudocolor) emissions are shown before or after YFP photobleach, as labeled.

occupancy governed by the concentration of the acceptor-tagged molecule and by the ratio of donor to acceptor (Hoppe et al., 2002; Zal and Gascoigne, 2004). Thus, the class of measurement typified by donor dequenching is affected by concentration of acceptor, and best used to track the donor occupancy by acceptor, whereas the class typified by sensitized emission (which must always correct for donor bleed-through into the acceptor measurement channel and direct excitation of acceptor at donor excitation wavelengths), is dependent on concentration of donor, and is best used to track acceptor occupancy by donor. To verify that the different FRET values are not due to such artifacts, or to "spurious FRET" arising from an increased abundance of neighboring fluorophores in the membrane (Erickson et al., 2003), we performed two types of analyses. The first was to quantify the ratio of donor to acceptor for each type of experiment by taking the ratios of the absolute intensities of CFP and YFP for each cell. From the measured CFP and YFP emission intensities from the CFP-YFP tandem construct we used as a positive control (which must be at a 1:1 ratio), we calibrated the ratio of CFP molecules to YFP molecules for each cell, and plotted the observed FRET as a function of CFP to YFP ratio on a cell-by-cell basis (supplemental Fig. 2, available at www.jneurosci.org as supplemental material). Using this analysis, we did find some significant differences between groups, but none that can account for the observed disruption in FRET efficiency for AKAP79/KCNQ2-5 interactions induced by WT CaM. The second was to back-calculate the observed FRET over a range of acceptor concentrations. As long as the acceptor is in excess, the measured FRET should not vary. Plotting the observed FRET as a function of YFP intensity also did not reveal any dependence of measured FRET on YFP intensity (data not shown), suggesting that the difference in FRET between the no CaM, WT CaM, and DN CaM groups for all of the KCNQ channels was not due to differing YFP expression levels.

Overexpression of a PIP_2 phosphatase does not disrupt the interaction between AKAP79$_{1-153}$ and KCNQ2-5 channels

PIP_2 is another molecule that is shared as being critical to the function of both KCNQ channels and AKAP79/150. For the former, PIP_2 is necessary for channel opening, and its depletion is a mechanism of channel inhibition (Delmas and Brown, 2005), and for the latter it has been postulated to be a major mechanism for plasma-membrane localization (Dell'Acqua et al., 1998). Thus, it is of interest to discover the influence of PIP_2 on AKAP79/150–channel interactions. As one initial test, we assayed the FRET between AKAP79$_{1-153}$ and KCNQ2-5 channels in cells depleted of PIP_2 by overexpression of a PIP_2 5-phosphatase, a maneuver shown to profoundly lower tonic PIP_2 levels (Raucher et al., 2000; Gamper et al., 2004; Li et al., 2005). Figure 4*A–D* shows examples of such experiments on cells cotransfected with CFP-tagged KCNQ2-5 subunits, AKAP79$_{1-153}$-YFP, and PIP_2 5-phosphatase, examined as above under TIRF microscopy using the donor-dequenching paradigm. The images report strong membrane abundance of AKAP79$_{1-153}$, even with PIP_2 depleted, and robust FRET for all four channel types. For KCNQ2-5, the FRET was 15.1 ± 1.8% (n = 14), 12.1 ± 2.5% (n = 17), 8.1 ± 2.5% (n = 11), and 16.1 ± 1.5% (n = 11), respectively, which are all not significantly less than the control values (Fig. 5). Figure 5 summarizes all the data testing interactions with AKAP79$_{1-153}$. In addition, shown are separate (positive) Rho-pYC and (negative) ECFP-M and AKAP79$_{1-153}$ control measurements. For all KCNQ2-5 channels, FRET reports substantial interaction with

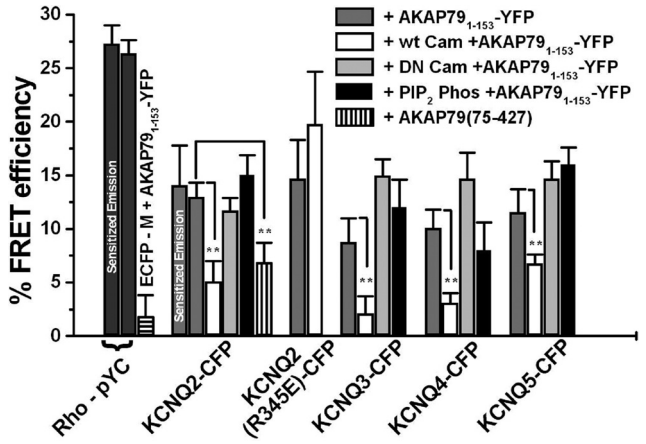

Figure 5. Summarized data for experiments involving AKAP79$_{1-153}$. Bars are summarized data for the groups of cells shown in Figure 4, as well as the FRET between CFP-tagged KCNQ2 and YFP-tagged AKAP79$_{1-153}$, or for Rho-pYC, measured using the sensitized-emission method.

full-length AKAP79 or AKAP79$_{1-153}$, although KCNQ2 is strongest. With an abundance of WT, but not DN, CaM, those interactions are severely disrupted for all the channels, most likely via CaM binding to the channels at an overlapping site with that of AKAP79. As for the CaM binding on AKAP79 that competes with PKC (Faux et al., 1999), Ca^{2+} is important since DN (apo) CaM has no effect. Finally, these interactions are not diminished in cells depleted of PIP_2.

PIP_2 depletion does not alter plasma-membrane localization of AKAP79

AKAP79 preferentially localizes to the plasma membrane, either when natively expressed in neurons or when heterologously expressed in mammalian cells. That membrane localization is also lost when the domains of AKAP79 necessary for PIP_2 binding are deleted, suggesting that membrane localization could be achieved via binding to anionic phospholipids (Dell'Acqua et al., 1998). Thus, we expected that the interactions between AKAP79 and KCNQ channels in the membrane would be disrupted in cells depleted of PIP_2 by overexpression of the PIP_2 5-phosphatase, but this was not the case. Thus, we set about to probe more systematically the dependence of AKAP79 localization on PIP_2 using several different approaches. As an initial test of our ability to determine the subcellular localization of AKAP79/150, we performed immunostaining experiments. CHO cells were cotransfected with (full-length) AKAP150 and GFP, fixed, and labeled with an anti-AKAP150 antibody (Santa Cruz Biotechnology). Slides were imaged using an Olympus FV500 confocal microscope housed in our Institutional Confocal Imaging Core. Shown in Figure 6*A* are confocal images from three such cells of GFP (left), AKAP150 (middle), or merged (right), confirming very strong tonic membrane localization of AKAP150. We then asked whether such membrane localization would change dynamically upon rapid depletion of membrane PIP_2 via two related methods. For both, the read-out is translocation of a membrane-bound fluorescent protein to the cytoplasm, observed via fast "swept-field" confocal (SFC) microscopy in individual living cells. The first was by stimulation of $G_{q/11}$-coupled M_1 receptors stably transfected in CHO cells and transfected with GFP-tagged AKAP79. As a control, cells were alternately transfected with a YFP-tagged PLCδ-PH construct that translocates from membrane to cytosol upon PIP_2 hydrolysis (Stauffer et al., 1998; Zhang et al., 2003; Gamper et al., 2004; Horowitz et al., 2005) or PIP_2 depletion (Suh et al., 2006; Varnai et al., 2006), thus providing optical verification of PIP_2 hydrolysis. Figure 6*B* shows representative experiments, including images before and after application of oxo-M (10 μM), and line-scan analyses. Before addition of agonist, GFP-AKAP79 is strongly localized to the membrane, consistent with the immunostaining results, and previous work (Dell'Acqua et al., 1998). Muscarinic stimulation did not induce any significant delocalization of GFP-AKAP79 from the membrane. That strong PIP_2 hydrolysis occurs in these experiments is confirmed in the cells transfected instead with YFP-PLCδ-PH, which displayed robust translocation from membrane to cytoplasm upon receptor stimulation. Such data are summarized in Figure 6*D*, plotted as the ratio of cytoplasmic fluorescence to that initially (F/F_0). For cells expressing GFP-AKAP79 or YFP-PLCδ-PH, F/F_0 values were 1.03 ± 0.04 ($n = 10$) and 2.71 ± 0.08 ($n = 10$), respectively. These results suggest that consumption of PIP_2 does not dynamically alter membrane AKAP79 localization.

However, since PIP_2 hydrolysis produces several downstream byproducts such as IP_3, Ca^{2+} signals, and diacylglycerol, and since the PLCδ-pH probes can only easily report PIP_2 hydrolysis, not PIP_2 depletion (Iino, 2000; Gamper et al., 2004; Winks et al., 2005), we turned to the chemically inducible dimerization (CID) strategy to directly deplete the membrane of PIP_2. CID exploits the binding of intracellular immunophilin proteins to a phosphoinositide 3-kinase related kinase involved in cell proliferation called mammalian target of rapamycin (mTOR) induced by the immunosuppressive compound rapamycin and its analogs. In particular rapamycin induces the dimerization of FK506 binding protein 12 (FKBP12) and the FKBP-rapamycin binding (FRB) domain of mTOR, this being the immunosuppressant mechanism of action of these drugs (Mita et al., 2003). Two groups have cleverly harnessed this chemically induced dimerization (CID) of FKBP and the FRB domains by fusing one (the FRB domain) with a membrane-localization tag from Lyn kinase (FRB-Lyn), and the other (FKBP) to both a fluorescent protein such as CFP and a PI kinase or PIP_2 phosphatase (Suh et al., 2006; Varnai et al., 2006). Upon addition of rapamycin or an analog to the bathing solution, CID occurs, bringing the kinase or phosphatase to the membrane, and membrane PIP_2 levels are thus either rapidly depressed or elevated. We used the CID method to suddenly deplete cell membranes of PIP_2 by cotransfection of a CFP-tagged FRB-Lyn and FKB12 fused to a PIP_2 phosphatase. Again, such cells were also cotransfected with either GFP-AKAP79 or with YFP-PLCδ-PH. In both cases, only cells clearly showing membrane-localized CFP fluorescence were selected for study. Figure 6*C* shows SFC images of cells before and 300 s after application of rapamycin (500 nM) to the bath. There was no delocalization of GFP-AKAP79 detected during this time, although the cells expressing YFP-PLCδ-PH confirm that strong PIP_2 depletion was occurring in these experiments. Such data are summarized in Figure 6*D*, plotted as the ratio of cytoplasmic fluorescence to that initially (F/F_0). For cells expressing GFP-AKAP79 or YFP-PLCδ-PH, F/F_0 values were 1.03 ± 0.03 ($n = 4$) and 2.38 ± 0.04 ($n = 4$). Thus, both experiments report that continued membrane localization of AKAP79 does not depend upon the presence or absence of PIP_2 in the membrane.

Calmodulin disrupts the functional effect of AKAP79 on heteromeric KCNQ2/3 channels

The TIRF/FRET data presented above suggest that high levels of functional CaM disrupt the physical interaction between KCNQ2-5

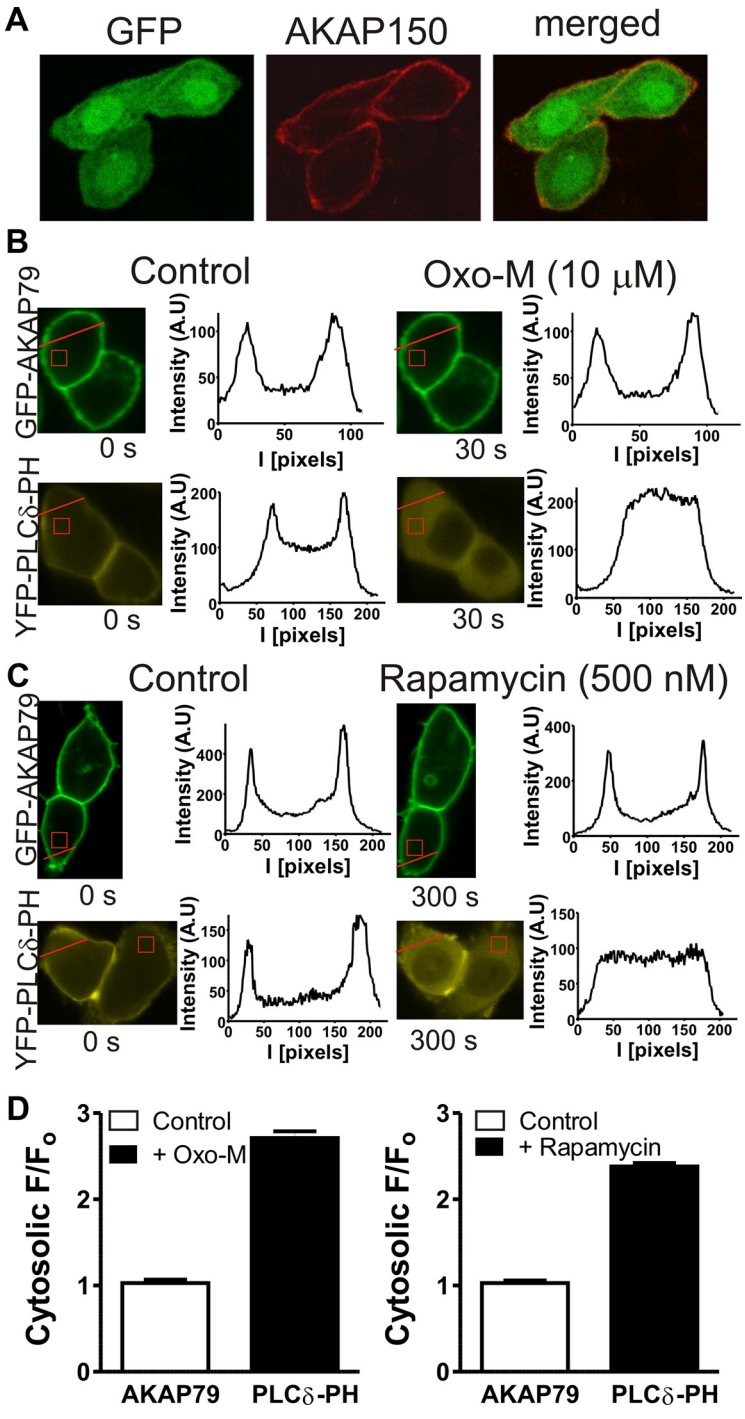

Figure 6. AKAP79/150 localization to the membrane is not dynamically altered by depletion of PIP_2. ***A***, Shown are conventional confocal images of CHO cells transfected with EGFP and AKAP150, fixed, and immunostained with anti-AKAP150 primary and anti-mouse Rhodamine Red secondary antibodies. Images were acquired either of GFP (using the 488 nm laser line), of Rhodamine Red (using the 543 laser line), or the merged image. ***B***, Shown are "swept-field" confocal images of stably expressing M_1 receptor CHO cells transfected with GFP-tagged AKAP79 or YFP-PH-PLCδPH, before or after bath application of oxo-M (10 μM). The images were analyzed either as a line scan or by quantifying the fluorescence in a cytoplasmic area (as shown). Shown in the insets are the results of the line scans for the presented images. Bars show summarized cytoplasmic F/F_0 data for all cells studied, where F_0 is the initial fluorescence. ***C***, Shown are "swept-field" confocal images of CHO cells transfected with the CFP-tagged FRB construct and untagged FKBP12 fused with a PIP_2 phosphatase, together with either GFP-tagged AKAP79 or YFP-PH-PLCδPH, before or after bath application of rapamycin (500 nM). The images were analyzed either as a line scan or by quantifying the fluorescence in a cytoplasmic area (as shown). Shown in the insets are the results of the line scans for the presented images. ***D***, Bars show summarized cytoplasmic F/F_0 data for all cells studied, where F_0 is the initial fluorescence.

channels and AKAP79. This result predicts that functional CaM should also disrupt the functional effect of AKAP79 on sensitivity of the channels to muscarinic stimulation, due to prevention of AKAP79-facilitated phosphorylation of the channels by PKC. To answer this question, we chose to examine the muscarinic sensitivity of heteromeric KCNQ2/3 channels, since they are the predominate correlate of neuronal M channels. In these experiments, we used two concentrations of oxo-M, 0.2 μM and 0.8 μM, concentrations that the previous experiments established to be near the IC_{50} for oxo-M-induced suppression of currents from heteromeric KCNQ2/3 channels cotransfected with GFP-tagged AKAP79, or with GFP only, respectively. Therefore, responses from these two concentrations of oxo-M should most accurately report changes in AKAP79 action on the channels.

In these experiments, cells stably expressing M_1 receptors were cotransfected with KCNQ2 + 3, together with either (1) GFP only, (2) GFP-tagged AKAP79, (3) GFP-tagged AKAP79 + WT CaM, or (4) GFP-tagged AKAP79 + DN CaM. The cells cotransfected with GFP-tagged AKAP79 displayed larger suppressions of the KCNQ2/3 current upon application of both 0.2 μM and 0.8 μM oxo-M, compared to cells cotransfected with GFP only (Fig. 7*A*,*B*), consistent with the results above that assayed the effect of AKAP79 on dose–response relations for KCNQ2/3 channels. However, this effect of AKAP79 was blocked in cells cotransfected with WT CaM, but there was no effect of cotransfection with DN CaM (Fig. 7*C*,*D*). These data are summarized in Figure 7*E*. For cells transfected with KCNQ2 + 3, together with GFP or with GFP-tagged AKAP79, the suppressions induced by 0.2 μM oxo-M were 22 ± 2% ($n = 3$) and 52 ± 4% ($n = 4$), respectively, and the suppressions induced by 0.8 μM oxo-M were 47 ± 1% ($n = 3$) and 84 ± 5% ($n = 4$), respectively. For cells expressing KCNQ2 + 3 and GFP-tagged AKAP79, together with WT or DN CaM, the suppressions induced by 0.2 μM were 21 ± 5% ($n = 4$) and 50 ± 6% ($n = 5$), respectively, and the suppressions induced by 0.8 μM oxo-M were 37 ± 7% ($n = 4$) and 82 ± 3% ($n = 5$), respectively. Thus, coexpression of WT, but not DN CaM, disrupts the functional effect on KCNQ2/3 channels mediated by AKAP79, likely due either to prevention of the physical interaction between AKAP79 and the channels, to blockade of PKC phosphorylation, or both.

Discussion

In this work, we show that AKAP79/150 actions generalize to KCNQ2-5 subtypes, involving intimate association of the scaffold proteins with the channels. The functional data are in accord with the TIRF/FRET measurements. From these results, we conclude that calcified CaM, but not apoCaM, disrupts the functional interactions between AKAP79 and M-type channels, likely due to CaM binding to the channels at an overlapping site with AKAP79/150. Although AKAP79/150 binds to PIP_2, as do KCNQ channels, tonic or acute depletion of PIP_2 did not affect the interaction of AKAP79 with KCNQ2-5, nor did it cause delocalization of AKAP79 from the plasma membrane. The current data with the KCNQ4 (T553A) mutant confirm the previous conclusion using KCNQ2 (Hoshi et al., 2003) that the AKAP79/150 action is indeed the mediation of phosphorylation of the channels by PKC. Our CaM data suggest a hypothesis to account for the receptor specificity for AKAP150 action in sympathetic neurons, in which a dominant-negative, RNA_i knockdown, or genetic knock-out of AKAP150 attenuated suppression of M current by muscarinic, but not bradykinin, receptor agonists (Hoshi et al., 2003, 2005; Tunquist et al., 2008). The hypothesis is based on the use of Ca^{2+}/CaM signals by bradykinin B_2, but not muscarinic M_1, receptors to suppress M current in SCG cells. Thus, the former, but not the latter, produce calcified CaM that binds to the channel, preventing AKAP79/150 interactions and subsequent PKC phosphorylation. We predict that M-current suppression by purinergic P2Y receptors, which also uses Ca^{2+}/CaM signals (Zaika et al., 2007), will also be insensitive to functional AKAP79/150, whereas angiotensin II AT1 receptor action on M channels, which parallels the muscarinic mechanism (Zaika et al., 2006), will be sensitized by AKAP79/150.

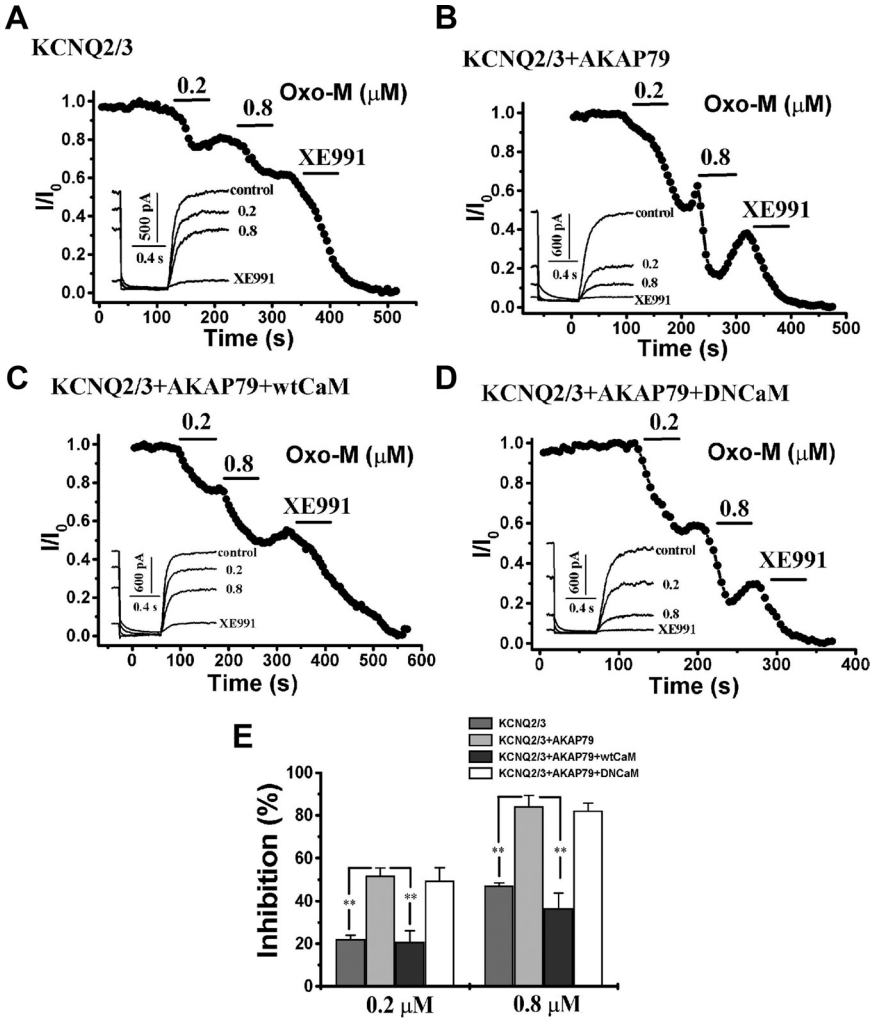

Figure 7. Functional, but not DN, CaM disrupts the AKAP79-mediated sensitization of KCNQ2/3 channels to inhibition by muscarinic receptor stimulation. Plotted are normalized KCNQ2/3 currents during the experiments from stably M_1-expressing CHO cells transfected with KCNQ2 + 3 and GFP only (***A***), KCNQ2 + 3 with GFP-tagged AKAP79 (***B***), KCNQ2 + 3 with GFP-tagged AKAP79 and WT CaM (***C***), or KCNQ2 + 3 with GFP-tagged AKAP79 and DN CaM (***D***), while oxo-M was bath applied at concentrations of 0.2 μM or 0.8 μM, as indicated by the bars. Representative current traces are shown in the insets, using the voltage protocol as in Figure 2. ***E***, Bars are summarized data for the groups of cells as in ***A–D***. $^{**}p < 0.01$.

Although AKAP79 does bind to PIP_2, and deletion of polybasic domains in the N terminus that overlap with those necessary for localization of AKAP79 to the membrane abrogates PIP_2 binding (Dell'Acqua et al., 1998), the presence of PIP_2 in the membrane per se seems not to be required for this localization, nor for interactions with KCNQ channels. Thus, when the cell membrane was depleted specifically of PIP_2, either tonically or acutely, there were no changes in membrane localization of AKAP79 in the membrane (Figs. 4, 6). This is probably not surprising since the large majority of domains that bind to PIP_2 display little specificity among negatively charged phospholipids (Kavran et al., 1998; Lemmon, 2003). Hence, domains within AKAP79/150 that can bind PIP_2 are also capable of binding to other acidic lipids, such as phosphatidylserine (Dell'Acqua et al., 1998). With regards to CaM action, our data suggest that CaM disrupts AKAP79/KCNQ-channel interactions by binding to the channels, but we cannot exclude CaM actions on AKAP79/150 as playing a role, such as that reported on membrane targeting or PKC activity (Dell'Acqua et al., 1998).

In nearly all cases, the protein complex orchestrated by AKAP proteins spans the cell-surface receptors used to initiate the signal, the protein kinase(s) involved, the channel targets, subcellular targeting molecules, and the phosphatases or phosphodiesterases used to terminate the intracellular event (Wong and Scott, 2004). For AKAP79/150 action on "L-type" (Ca_v1) Ca^{2+} channels, the dynamics are even more complex, since the Ca^{2+} ions that enter the cell through the channels themselves feed back on the phosphorylation complex via the Ca^{2+} and CaM-regulated phosphatase calcineurin, supporting an activity-dependent constraint on AKAP79/150 actions (Hall et al., 2007; Oliveria et al., 2007). Moreover, since activity of $Ca_v1.2$ channels also controls the transcription of Ca^{2+}-sensitive genes (Dolmetsch, 2003; Gomez-Ospina et al., 2006), the reach of this scaffold protein extends into the nucleus, and to the long-term agenda of the cell, and of highly plastic phenomena, such as dendrite and memory

formation in the brain (Hoogland and Saggau, 2004; Lu et al., 2008; Tunquist et al., 2008). Thus, the events co-coordinated by AKAP proteins range temporally over many orders of magnitude, from the second to the lifetime of the organism.

Recent work indicates that the apparent affinity of PIP_2 for KCNQ1-5 channels is quite variable, with the channels being characterized as having high PIP_2 affinity, rendering the channels less sensitive to changes in PIP_2 abundance, or having low PIP_2 affinity, endowing them with high sensitivity to physiological changes in [PIP_2], such as that caused by stimulation of M_1 receptors in neurons (Selyanko et al., 2001; Li et al., 2004, 2005; Hernandez et al., 2008). We recently adapted an earlier cellular model used to simulate muscarinic depression of M current via PIP_2 metabolism (Suh et al., 2004) to reproduce the variable sensitivity seen among KCNQ channels to inhibition by muscarinic receptor stimulation. That model correctly simulated high-affinity KCNQ3 channels to be only modestly inhibited by saturating stimulation of M_1 receptors stably expressed in CHO cells (the same system used here), whereas low-affinity KCNQ2 and KCNQ4 channels were predicted to be profoundly inhibited at saturating concentrations, with IC_{50} values for oxo-M shifted to much lower concentrations, relative to KCNQ2/3 heteromers. Our data in this paper are wholly consistent with that modeling, and with AKAP79/150-recruited PKC phosphorylation of KCNQ2-5 decreasing their affinity for PIP_2, with differing effects on the oxo-M dose–response relation dependent on the PIP_2 affinity of the channels. Thus, cotransfection of AKAP79 with KCNQ2, KCNQ4, or KCNQ5 shifted the dose–response curves of [oxo-M] versus channel inhibition to lower concentrations, whereas the presence of AKAP79 resulted in a dramatic increase in the inhibition of KCNQ3 at saturating [oxo-M], with only a small shift in the IC_{50} value. Functionally, AKAP79/150-PKC therefore acts to "convert" high PIP_2-affinity channels with low muscarinic sensitivity to lower PIP_2-affinity channels with higher muscarinic sensitivity, thus "priming" or sensitizing them to physiological stimulation of receptors (Gamper and Shapiro, 2007b). This phenomenon has strong parallels with the situation for PIP_2-sensitive Kir channels, for which diverse intracellular signaling molecules act by altering the affinity of PIP_2 for the channels, sensitizing them to small or local changes in PIP_2 abundance (Logothetis et al., 2007).

How much does AKAP79/150-PKC lower the affinity of the different KCNQ channels for PIP_2? We can use the parameters of our recent model to provide some quantitative estimates (Hernandez et al., 2009). That model contains several basic steps of the cascade that all use first-order rate constants. The first combines muscarinic receptor binding by oxo-M, $G_{q/11}$ activation and PLC stimulation into one reaction describing agonist-dependent activation of PLC molecules. The second uses rate constants for PIP_2 synthesis by PI-kinases and hydrolysis of PIP_2 by activated PLC. The third contains binding/unbinding of PIP_2 to/from KCNQ subunits governed by a simple association constant, K_A, that is specific for each type of subunit. This model allows direct conversion of changes in the IC_{50} for muscarinic depression of the KCNQ current to changes in the K_A of PIP_2 for a channel subunit, since $\log(K_A)$ will scale linearly with $\log(IC_{50})$. Using linear interpolations of the model outputs over a wide range of K_A values (75–9600 molecules/μm^2) (Hernandez et al., 2009, their supplemental Fig. S1*A*), we estimated the effects of cotransfection of AKAP79 on each channel. For KCNQ2-5 homomers, the presence of AKAP79 decreased the predicted K_A values by 11.6-fold, 3.1-fold, 5.3-fold, and 5.8-fold, respectively. Hoshi et al. (2003) showed PKC to phosphorylate KCNQ2 at two sites in the C terminus, S534 and S541. Interestingly, among KCNQ2-5 subunits, KCNQ2 uniquely possesses a serine or threonine at both positions, whereas KCNQ3-5 have other residues at the 534 position. This difference strikingly parallels the approximately twofold larger effect on the K_A value predicted for KCNQ2, versus the others. For KCNQ3, the predicted effect, as taken from the change in IC_{50}, is a little smaller than the others, but for that high PIP_2-affinity channel, a decrease in PIP_2 affinity is better manifested by the increase in the inhibition at saturating agonist, and that effect was large in the data. Thus, the predicted effect of AKAP79 on the K_A of PIP_2 for KCNQ3 subunit is probably about the same as for KCNQ4 or KCNQ5. For KCNQ2/3 heteromers (Fig. 2), the same quantification suggests the overall PIP_2 affinity to be reduced by 10.8-fold by AKAP79, indistinguishable to that for KCNQ2 homomers. Why should that be? Again, the recent modeling yields the likely answer, since the high PIP_2 affinity of KCNQ3 subunits means that PIP_2 will usually remain bound, even at saturating receptor stimulation (Hernandez et al., 2009). Thus, in the heteromeric channel, it is the PIP_2 occupancy of the KCNQ2 subunits that probably acts as the master switch governing activity of the overall tetrameric channel, predicting that changes in PIP_2 affinity induced by PKC phosphorylation of those subunits will determine the overall effect on heteromeric KCNQ2/3 channel function. The present discussion should stimulate some useful thinking. However, it will require biochemical analyses of channel/PIP_2 affinities, and the analytical determination of changes in those affinities induced by signaling events, such as PKC phosphorylation, to make definitive conclusions about the biochemical and kinetic mechanisms underlying AKAP79/150 action on the channels. In addition, our inquiry here focused on interactions between heterologously expressed cloned channels and cloned AKAP molecules, whereas investigations on endogenous proteins will be required to confirm these findings in the milieu of native neurons. We look forward to such analyses.

References

Axelrod D (2003) Total internal reflection fluorescence microscopy in cell biology. Methods Enzymol 361:1–33.

Bal M, Zaika O, Martin P, Shapiro MS (2008) Calmodulin binding to M-type K^+ channels assayed by TIRF/FRET in living cells. J Physiol 586:2307–2320.

Centonze VE, Sun M, Masuda A, Gerritsen H, Herman B (2003) Fluorescence resonance energy transfer imaging microscopy. Methods Enzymol 360:542–560.

Chen L, Kurokawa J, Kass RS (2005) Phosphorylation of the A-kinase-anchoring protein Yotiao contributes to protein kinase A regulation of a heart potassium channel. J Biol Chem 280:31347–31352.

Coghlan VM, Perrino BA, Howard M, Langeberg LK, Hicks JB, Gallatin WM, Scott JD (1995) Association of protein kinase A and protein phosphatase 2B with a common anchoring protein. Science 267:108–111.

Dell'Acqua ML, Faux MC, Thorburn J, Thorburn A, Scott JD (1998) Membrane-targeting sequences on AKAP79 bind phosphatidylinositol-4, 5-bisphosphate. EMBO J 17:2246–2260.

Delmas P, Brown DA (2005) Pathways modulating neural KCNQ/M (Kv7) potassium channels. Nat Rev Neurosci 6:850–862.

Dolmetsch R (2003) Excitation-transcription coupling: signaling by ion channels to the nucleus. Sci STKE 2003:PE4.

Erickson MG, Alseikhan BA, Peterson BZ, Yue DT (2001) Preassociation of calmodulin with voltage-gated Ca^{2+} channels revealed by FRET in single living cells. Neuron 31:973–985.

Erickson MG, Moon DL, Yue DT (2003) DsRed as a potential FRET partner with CFP and GFP. Biophys J 85:599–611.

Faux MC, Scott JD (1997) Regulation of the AKAP79-protein kinase C interaction by Ca^{2+}/calmodulin. J Biol Chem 272:17038–17044.

Faux MC, Rollins EN, Edwards AS, Langeberg LK, Newton AC, Scott JD

(1999) Mechanism of A-kinase-anchoring protein 79 (AKAP79) and protein kinase C interaction. Biochem J 343:443–452.

Fowler CE, Aryal P, Suen KF, Slesinger PA (2007) Evidence for association of $GABA_B$ receptors with Kir3 channels and regulators of G protein signalling (RGS4) proteins. J Physiol 580:51–65.

Gamper N, Shapiro MS (2003) Calmodulin mediates Ca^{2+}-dependent modulation of M-type K^+ channels. J Gen Physiol 122:17–31.

Gamper N, Shapiro MS (2007a) Regulation of ion transport proteins by membrane phosphoinositides. Nat Rev Neurosci 8:921–934.

Gamper N, Shapiro MS (2007b) Target-specific PIP_2 signalling: how might it work? J Physiol 582:967–975.

Gamper N, Reznikov V, Yamada Y, Yang J, Shapiro MS (2004) Phosphatidylinositol 4,5-bisphosphate signals underlie receptor-specific $G_{q/11}$-mediated modulation of N-type Ca^{2+} channels. J Neurosci 24: 10980–10992.

Gamper N, Li Y, Shapiro MS (2005a) Structural requirements for differential sensitivity of KCNQ K^+ channels to modulation by Ca^{2+}/calmodulin. Mol Biol Cell 16:3538–3551.

Gamper N, Stockand JD, Shapiro MS (2005b) The use of Chinese hamster ovary (CHO) cells in the study of ion channels. J Pharmacol Toxicol Methods 51:177–185.

Geiser JR, van Tuinen D, Brockerhoff SE, Neff MM, Davis TN (1991) Can calmodulin function without binding calcium? Cell 65:949–959.

Gomez-Ospina N, Tsuruta F, Barreto-Chang O, Hu L, Dolmetsch R (2006) The C terminus of the L-type voltage-gated calcium channel $Ca_V1.2$ encodes a transcription factor. Cell 127:591–606.

Gordon GW, Berry G, Liang XH, Levine B, Herman B (1998) Quantitative fluorescence resonance energy transfer measurements using fluorescence microscopy. Biophys J 74:2702–2713.

Haitin Y, Attali B (2008) The C-terminus of Kv7 channels: a multifunctional module. J Physiol 586:1803–1810.

Hall DD, Davare MA, Shi M, Allen ML, Weisenhaus M, McKnight GS, Hell JW (2007) Critical role of cAMP-dependent protein kinase anchoring to the L-type calcium channel Cav1.2 via A-kinase anchor protein 150 in neurons. Biochemistry 46:1635–1646.

Hernandez CC, Zaika O, Shapiro MS (2008) A carboxy-terminal inter-helix linker as the site of phosphatidylinositol 4,5-bisphosphate action on Kv7 (M-type) K^+ channels. J Gen Physiol 132:361–381.

Hernandez CC, Falkenburger B, Shapiro MS (2009) Affinity for phosphatidylinositol 4,5-bisphosphate determines muscarinic agonist sensitivity of Kv7 K^+ channels. J Gen Physiol 134:437–448.

Hille B (1994) Modulation of ion-channel function by G-protein-coupled receptors. Trends Neurosci 17:531–536.

Hirsch AH, Glantz SB, Li Y, You Y, Rubin CS (1992) Cloning and expression of an intron-less gene for AKAP 75, an anchor protein for the regulatory subunit of cAMP-dependent protein kinase II beta. J Biol Chem 267:2131–2134.

Hoogland TM, Saggau P (2004) Facilitation of L-type Ca^{2+} channels in dendritic spines by activation of beta2 adrenergic receptors. J Neurosci 24:8416–8427.

Hoppe A, Christensen K, Swanson JA (2002) Fluorescence resonance energy transfer-based stoichiometry in living cells. Biophys J 83:3652–3664.

Horowitz LF, Hirdes W, Suh BC, Hilgemann DW, Mackie K, Hille B (2005) Phospholipase C in living cells: activation, inhibition, Ca^{2+} requirement, and regulation of M current. J Gen Physiol 126:243–262.

Hoshi N, Zhang JS, Omaki M, Takeuchi T, Yokoyama S, Wanaverbecq N, Langeberg LK, Yoneda Y, Scott JD, Brown DA, Higashida H (2003) AKAP150 signaling complex promotes suppression of the M-current by muscarinic agonists. Nat Neurosci 6:564–571.

Hoshi N, Langeberg LK, Scott JD (2005) Distinct enzyme combinations in AKAP signalling complexes permit functional diversity. Nat Cell Biol 7:1066–1073.

Iino M (2000) Molecular basis of spatio-temporal dynamics in inositol 1,4,5-trisphosphate-mediated Ca^{2+} signalling. Jpn J Pharmacol 82: 15–20.

Kavran JM, Klein DE, Lee A, Falasca M, Isakoff SJ, Skolnik EY, Lemmon MA (1998) Specificity and promiscuity in phosphoinositide binding by pleckstrin homology domains. J Biol Chem 273:30497–30508.

Klauck TM, Faux MC, Labudda K, Langeberg LK, Jaken S, Scott JD (1996) Coordination of three signaling enzymes by AKAP79, a mammalian scaffold protein. Science 271:1589–1592.

Lemmon MA (2003) Phosphoinositide recognition domains. Traffic 4:201–213.

Li Y, Gamper N, Shapiro MS (2004) Single-channel analysis of KCNQ K^+ channels reveals the mechanism of augmentation by a cysteine-modifying reagent. J Neurosci 24:5079–5090.

Li Y, Gamper N, Hilgemann DW, Shapiro MS (2005) Regulation of Kv7 (KCNQ) K^+ channel open probability by phosphatidylinositol (4,5)-bisphosphate. J Neurosci 25:9825–9835.

Logothetis DE, Lupyan D, Rosenhouse-Dantsker A (2007) Diverse Kir modulators act in close proximity to residues implicated in phosphoinositide binding. J Physiol 582:953–965.

Lu Y, Zhang M, Lim IA, Hall DD, Allen M, Medvedeva Y, McKnight GS, Usachev YM, Hell JW (2008) AKAP150-anchored PKA activity is important for LTD during its induction phase. J Physiol 586:4155–4164.

Mita MM, Mita A, Rowinsky EK (2003) The molecular target of rapamycin (mTOR) as a therapeutic target against cancer. Cancer Biol Ther 2:S169–177.

Oliveria SF, Gomez LL, Dell'Acqua ML (2003) Imaging kinase—AKAP79—phosphatase scaffold complexes at the plasma membrane in living cells using FRET microscopy. J Cell Biol 160:101–112.

Oliveria SF, Dell'Acqua ML, Sather WA (2007) AKAP79/150 anchoring of calcineurin controls neuronal L-type Ca^{2+} channel activity and nuclear signaling. Neuron 55:261–275.

Patterson G, Day RN, Piston D (2001) Fluorescent protein spectra. J Cell Sci 114:837–838.

Rae J, Cooper K, Gates P, Watsky M (1991) Low access resistance perforated patch recordings using amphotericin B. J Neurosci Methods 37:15–26.

Raucher D, Stauffer T, Chen W, Shen K, Guo S, York JD, Sheetz MP, Meyer T (2000) Phosphatidylinositol 4,5-bisphosphate functions as a second messenger that regulates cytoskeleton-plasma membrane adhesion. Cell 100:221–228.

Robbins J, Marsh SJ, Brown DA (2006) Probing the regulation of M (Kv7) potassium channels in intact neurons with membrane-targeted peptides. J Neurosci 26:7950–7961.

Sekar RB, Periasamy A (2003) Fluorescence resonance energy transfer (FRET) microscopy imaging of live cell protein localizations. J Cell Biol 160:629–633.

Selyanko AA, Hadley JK, Brown DA (2001) Properties of single M-type KCNQ2/KCNQ3 potassium channels expressed in mammalian cells. J Physiol 534:15–24.

Sorkin A, McClure M, Huang F, Carter R (2000) Interaction of EGF receptor and grb2 in living cells visualized by fluorescence resonance energy transfer (FRET) microscopy. Curr Biol 10:1395–1398.

Stauffer TP, Ahn S, Meyer T (1998) Receptor-induced transient reduction in plasma membrane PtdIns(4,5)P2 concentration monitored in living cells. Curr Biol 8:343–346.

Steyer JA, Almers W (2001) A real-time view of life within 100 nm of the plasma membrane. Nat Rev Mol Cell Biol 2:268–275.

Suh BC, Hille B (2002) Recovery from muscarinic modulation of M current channels requires phosphatidylinositol 4,5-bisphosphate synthesis. Neuron 35:507–520.

Suh BC, Horowitz LF, Hirdes W, Mackie K, Hille B (2004) Regulation of KCNQ2/KCNQ3 current by G-protein cycling: the kinetics of receptor-mediated signaling by Gq. J Gen Physiol 123:663–683.

Suh BC, Inoue T, Meyer T, Hille B (2006) Rapid chemically induced changes of PtdIns(4,5)P2 gate KCNQ ion channels. Science 314:1454–1457.

Tunquist BJ, Hoshi N, Guire ES, Zhang F, Mullendorff K, Langeberg LK, Raber J, Scott JD (2008) Loss of AKAP150 perturbs distinct neuronal processes in mice. Proc Natl Acad Sci U S A 105:12557–12562.

Varnai P, Thyagarajan B, Rohacs T, Balla T (2006) Rapidly inducible changes in phosphatidylinositol 4,5-bisphosphate levels influence multiple regulatory functions of the lipid in intact living cells. J Cell Biol 175:377–382.

Wen H, Levitan IB (2002) Calmodulin is an auxiliary subunit of KCNQ2/3 potassium channels. J Neurosci 22:7991–8001.

Winks JS, Hughes S, Filippov AK, Tatulian L, Abogadie FC, Brown DA, Marsh SJ (2005) Relationship between membrane phosphatidylinositol-4,5-

bisphosphate and receptor-mediated inhibition of native neuronal M channels. J Neurosci 25:3400–3413.

Wong W, Scott JD (2004) AKAP signalling complexes: focal points in space and time. Nat Rev Mol Cell Biol 5:959–970.

Yus-Najera E, Santana-Castro I, Villarroel A (2002) The identification and characterization of a non-continuous calmodulin binding site in non-inactivating voltage-dependent KCNQ potassium channels. J Biol Chem 277:28545–28553.

Zaika O, Lara LS, Gamper N, Hilgemann DW, Jaffe DB, Shapiro MS (2006) Angiotensin II regulates neuronal excitability via phosphatidylinositol 4,5-bisphosphate-dependent modulation of Kv7 (M-type) K^+ channels. J Physiol 575:49–67.

Zaika O, Tolstykh GP, Jaffe DB, Shapiro MS (2007) Inositol triphosphate-mediated Ca^{2+} signals direct purinergic P2Y-receptor regulation of neuronal ion channels. J Neurosci 27:8914–8926.

Zaika O, Hernandez CC, Bal M, Tolstykh GP, Shapiro MS (2008) Determinants within the turret and pore-loop domains of KCNQ3 K^+ channels governing functional activity. Biophys J 95:5121–5137.

Zal T, Gascoigne NR (2004) Photobleaching-corrected FRET efficiency imaging of live cells. Biophys J 86:3923–3939.

Zhang H, Craciun LC, Mirshahi T, Rohács T, Lopes CM, Jin T, Logothetis DE (2003) PIP_2 activates KCNQ channels, and its hydrolysis underlies receptor-mediated inhibition of M currents. Neuron 37:963–975.

Zheng J, Zagotta WN (2004) Stoichiometry and assembly of olfactory cyclic nucleotide-gated channels. Neuron 42:411–421.